

# Supplementary Material for “Dielectric modulation of two-dimensional dipolar materials”

Ziwei Wang<sup>1</sup> and Erik Luijten<sup>1,2,\*</sup>

<sup>1</sup>Graduate Program in Applied Physics, Northwestern University, Evanston, Illinois 60208, U.S.A.

<sup>2</sup>Departments of Materials Science & Engineering, Engineering Sciences & Applied Mathematics, and Physics & Astronomy, Northwestern University, Evanston, Illinois 60208, U.S.A.

## REFORMULATION OF THE HAMILTONIAN AND PHASE DIAGRAM

We discuss an alternate representation of the Hamiltonian as well as the phase diagram constructed under this representation. The Hamiltonian presented in the main text can be written as

$$\frac{\mathcal{H}}{k_B T} = \frac{1}{2} \sum_{i=1}^N \sum_{\mathbf{n}} \left\{ \lambda_{\text{dd}} \sum_{j=1}^N \frac{\hat{\boldsymbol{\mu}}_i \cdot \hat{\boldsymbol{\mu}}_j - 3(\hat{\boldsymbol{\mu}}_i \cdot \hat{\mathbf{r}}_{ij}^{\text{rep}})(\hat{\boldsymbol{\mu}}_j \cdot \hat{\mathbf{r}}_{ij}^{\text{rep}})}{|\hat{\mathbf{r}}_{ij}^{\text{rep}}|^3} + \gamma \lambda_{\text{dd}} \sum_{j=1}^N \frac{\hat{\boldsymbol{\mu}}_i \cdot \hat{\boldsymbol{\mu}}'_j - 3(\hat{\boldsymbol{\mu}}_i \cdot \hat{\mathbf{r}}_{ij}^{\text{rep}})(\hat{\boldsymbol{\mu}}'_j \cdot \hat{\mathbf{r}}_{ij}^{\text{rep}})}{|\alpha^2 + |\hat{\mathbf{r}}_{ij}^{\text{rep}}|^2|^{3/2}} \right\},$$

in which all variables have been introduced in the main text. In this formulation, we choose the dielectric mismatch  $\gamma$  as an independent variable rather than  $\lambda_{\text{di}}$ . There are two motivations for adopting this representation. First,  $\gamma$  is more directly related to materials properties, thus facilitating the connection to experiments. Second, in the long-range limit ( $|\hat{\mathbf{r}}_{ij}^{\text{rep}}| \gg \alpha$ ) the total dipole–image energy scales as  $\gamma \lambda_{\text{dd}}$  compared to the dipole–dipole energy, which scales as  $\lambda_{\text{dd}}$ . Therefore,  $\gamma$  measures the anisotropy of the effective long-range interaction. However, we remark that  $\gamma$  only determines the *magnitude* of the dipole–image energy relative to the total long-range energy. Whether this contribution will reinforce or counteract the dipole–dipole energy is different for dipoles with in-plane and out-of-plane orientation.

In addition to  $\lambda_{\text{dd}}$ , which serves as a global energy scale (or inverse temperature), and  $\gamma$ , we choose  $\alpha$  as the third independent parameter.  $\alpha$  determines the magnitude of the surface anisotropy (i.e., the first-order dipole–image interaction), characterized by  $\gamma \lambda_{\text{dd}}/\alpha^3$ . Figure S1 shows a  $\lambda_{\text{dd}} = 5$  section of the phase diagram in the  $\alpha$ – $\gamma$  plane.

## ENERGY ANALYSIS OF THE MODULATED PHASES

We (i) derive the effective pairwise potential between two dipoles placed on a dielectric substrate and (ii) demonstrate how this potential affects the resultant modulated phases. As a representative example, we focus on the stripe phase ( $\lambda_{\text{di}} < 0$ ,  $\gamma < 0$ ) and assume that the dipole moments of the particles are oriented perpendicular to the substrate owing to the attraction by their own images (cf. Fig. 4a, main text). Thus, the dipole moment  $\boldsymbol{\mu}_i$  of particle  $i$  is given by  $\boldsymbol{\mu}_i = \mu \boldsymbol{\sigma}_i$ , where

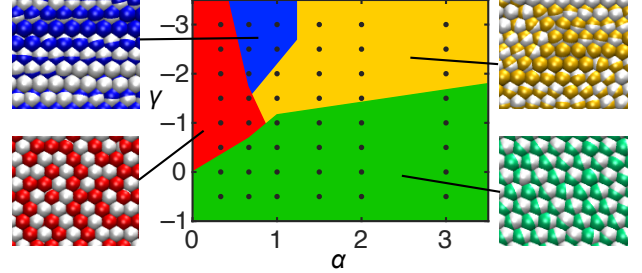


FIG. S1. Phase diagram parametrized by  $\alpha$  and  $\gamma$  at  $\lambda_{\text{dd}} = 5$ . Phase boundaries are drawn based on discrete simulation data points with positions indicated by the black dots.

$\boldsymbol{\sigma}_i = (0, 0, \sigma_{i,z}) = (0, 0, \pm 1)$ . The induced image dipole is  $\boldsymbol{\mu}'_i = -\gamma \mu \boldsymbol{\sigma}_i$  (with  $\gamma$  as defined in the main text).

The electric field at the position  $\mathbf{r}_j$  of dipole  $j$ , generated by dipole  $i$  located at  $\mathbf{r}_i$  and its image located at  $\mathbf{r}'_i = \mathbf{r}_i - (0, 0, d)$  (we recall that all dipoles are located at a distance  $d/2$  above the surface) is

$$\mathbf{E}(\boldsymbol{\sigma}_i, r_{ij}) = \mathbf{E}^{\text{dd}}(\boldsymbol{\sigma}_i, r_{ij}) + \mathbf{E}^{\text{di}}(\boldsymbol{\sigma}_i, r_{ij}), \quad (1)$$

where  $r_{ij} = |\mathbf{r}_{ij}| = |\mathbf{r}_j - \mathbf{r}_i|$ . Here the contributions  $\mathbf{E}^{\text{dd}}$  of the real dipole and  $\mathbf{E}^{\text{di}}$  of the image dipole are expressed as

$$\mathbf{E}^{\text{dd}}(\boldsymbol{\sigma}_i, r_{ij}) = -\frac{\mu \boldsymbol{\sigma}_i}{\epsilon_m r_{ij}^3}, \quad (2)$$

$$\mathbf{E}^{\text{di}}(\boldsymbol{\sigma}_i, r_{ij}) = \frac{\gamma \mu}{\epsilon_m} \left( \frac{\boldsymbol{\sigma}_i}{(r_{ij}^2 + d^2)^{3/2}} - \frac{3d \sigma_{i,z} \mathbf{r}'_{ij}}{(r_{ij}^2 + d^2)^{5/2}} \right), \quad (3)$$

where  $\mathbf{r}'_{ij} = \mathbf{r}_j - \mathbf{r}'_i = \mathbf{r}_{ij} + (0, 0, d)$ . Thus, the total pairwise electrostatic energy between dipole  $i$  and  $j$  is

$$U_{\text{p}}^{\text{tot}}(\boldsymbol{\sigma}_i, \boldsymbol{\sigma}_j, r_{ij}) = -\boldsymbol{\mu}_j \cdot \mathbf{E}(\boldsymbol{\sigma}_i, r_{ij}) = U_{\text{p}}^{\text{dd}} + U_{\text{p}}^{\text{di}}, \quad (4)$$

where the dipole–dipole and dipole–image (i.e., interaction of a dipole with the polarization induced by the *other* dipole) contributions,  $U_{\text{p}}^{\text{dd}}$  and  $U_{\text{p}}^{\text{di}}$ , are given by

$$\frac{U_{\text{p}}^{\text{dd}}(\boldsymbol{\sigma}_i, \boldsymbol{\sigma}_j, \tilde{r}_{ij})}{k_B T} = \lambda_{\text{dd}} \frac{\sigma_{i,z} \sigma_{j,z}}{\tilde{r}_{ij}^3}, \quad (5)$$

$$\frac{U_{\text{p}}^{\text{di}}(\boldsymbol{\sigma}_i, \boldsymbol{\sigma}_j, \tilde{r}_{ij})}{k_B T} = \lambda_{\text{di}} \left( \frac{2\alpha^2 - \tilde{r}_{ij}^2}{\alpha^2 + \tilde{r}_{ij}^2} \right) \frac{\sigma_{i,z} \sigma_{j,z}}{(1 + \tilde{r}_{ij}^2/\alpha^2)^{3/2}}. \quad (6)$$

As in the main text, we choose the lattice constant  $a$  as the unit length and use a tilde to denote reduced lengths.

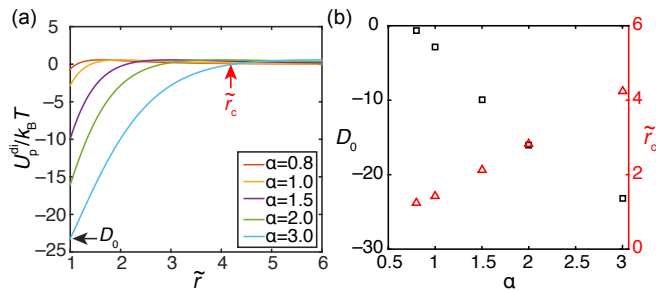


FIG. S2. Illustration of the effective pairwise interaction between two dipoles placed on a dielectric substrate and oriented parallel to the  $z$ -axis. As in Fig. 4 in the main text, we set  $\lambda_{\text{dd}} = 5$  and  $\lambda_{\text{di}} = -16$ , corresponding to the stripe phase. (a) Dipole–image component of the pairwise interaction,  $U_{\text{p}}^{\text{di}}$ , as a function of the center-to-center distance  $\tilde{r}$  at different values of the geometric factor  $\alpha$ . The depth  $D_0$  of the energy well and the critical separation  $\tilde{r}_c$  at which  $U_{\text{p}}^{\text{di}}$  switches sign are marked by arrows. (b) Dependence of the two characteristic parameters  $D_0$  (left-hand axis) and  $\tilde{r}_c$  (right-hand axis) as functions of  $\alpha$ . Both quantities grow in magnitude with increasing  $\alpha$ .

From the energy expressions Eqs. (5) and (6) it is evident that the magnitudes of both  $U_{\text{p}}^{\text{dd}}$  and  $U_{\text{p}}^{\text{di}}$  decay asymptotically with the center-to-center distance  $\tilde{r}$  as  $1/\tilde{r}^3$ . However, what truly matters is how these interactions depend, at different length scales, on the relative dipolar orientations  $\{\sigma_{i,z}, \sigma_{j,z}\}$ . The direct interaction  $U_{\text{p}}^{\text{dd}}$  decays monotonically, favoring anti-parallel orientational arrangements (with  $\sigma_{i,z}\sigma_{j,z} = -1$ ) at all length scales. However, at sufficiently short  $\tilde{r}$  this is overwhelmed by the deep energy well of the dipole–image interaction  $U_{\text{p}}^{\text{di}}$  with  $\sigma_{i,z}\sigma_{j,z} = 1$  (Fig. S2a), favoring parallel arrangements. At  $\tilde{r}_c = \sqrt{2}\alpha$ , the dipole–image contribution changes sign, so that a nonmonotonic trend results, where ferroelectric order is preferred at short distances and anti-parallel

arrangements become favorable at larger  $\tilde{r}$ . Thus, as illustrated in the main text, the dipole–image component of the pairwise interaction acts as an effective ‘exchange interaction’ to promote short-range ferroelectricity. Here the depth of the energy well  $D_0 = \lambda_{\text{di}}^{(2)} \frac{2\alpha^2 - 1}{\alpha^2 + 1}$  (in reduced units) and the critical distance  $\tilde{r}_c$  at which  $U_{\text{p}}^{\text{di}}$  switches sign characterize the strength and range of this exchange interaction, both of which grow in magnitude with  $\alpha$  (Fig. S2b).

Interestingly, even though the interaction range extends beyond the nearest neighbors (especially at large  $\alpha$ ), we observe that the exponential dependence of the stripe width on the exchange parameter, as found for the 2D dipolar Ising system [1] (with nearest-neighbor exchange interaction only), accurately describes our system as well (see Fig. 4b in the main text).

Finally, it is noteworthy that while the observed orientational phases can be realized in magnetic films by exploiting the quantum exchange interaction, they cannot be sustained in systems with larger length scales (e.g., in colloidal systems). By contrast, in the approach proposed here the many-body dielectric force acts effectively as an exchange interaction in which both strength and range can be tuned independently by varying  $\lambda_{\text{di}}$  and  $\alpha$ . This provides new ways to realize and control orientationally modulated patterns beyond the atomic scale, with potential applications in optical devices and the possibility to serve as a starting point for other studies on controlling orientational structure in materials.

---

\* Corresponding author: [luijten@northwestern.edu](mailto:luijten@northwestern.edu)  
 [1] A. B. Maclsaac, J. P. Whitehead, M. C. Robinson, and K. De’Bell, “Striped phases in two-dimensional dipolar ferromagnets,” *Phys. Rev. B* **51**, 16033–16045 (1995).